Molecular Microbiology (2001) **40**(3), 744–756

The *act* operon controls the level and time of C-signal production for *Myxococcus xanthus* development

Thomas M. A. Gronewold and Dale Kaiser*
Departments of Biochemistry and Developmental Biology, Stanford University School of Medicine, 297 Campus Drive, Stanford, CA 94305, USA.

Summary

The C-signal is a morphogen that controls the assembly of fruiting bodies and the differentiation of myxospores. Production of this signal, which is encoded by the *csg*A gene, is regulated by the *act* operon of four genes that are co-transcribed from the same start site. The *act*A and *act*B genes regulate the maximum level of the C-signal, which never rises above one-quarter of the maximum wild-type level of CsgA protein in null mutants of either gene. The *act*A and *act*B mutants have the same developmental phenotype: both aggregate, neither sporulates, both prolong rippling. By sequence homology, *act*A encodes a response regulator, and *act*B encodes a sigma-54 activator protein of the NTRC class. The similar phenotypes of *act*A and *act*B deletion mutants suggest that the two gene products are part of the same signal transduction pathway. That pathway responds to C-signal and also regulates the production of CsgA protein, thus creating a positive feedback loop. The *act*C and *act*D genes regulate the time pattern of CsgA production, while achieving the same maximum level. An *act*C null mutant raises CsgA production 15 h earlier than the wild type, whereas an *act*D null mutant does so 6 h later than wild type. The loop explains how the C-signal rises continuously from early development to a peak at the time of sporulation, and the *act* genes govern the time course of that rise.

Introduction

Myxobacteria develop their organized multicellular fruiting bodies in response to starvation (Dworkin, 1996; Harris *et al*., 1998). Although the fruiting body of *Myxococcus xanthus* is a relatively simple hemispherical mound filled with spores, its formation nevertheless involves the co-ordination of cell movement and cell differentiation characteristic of many developmental processes, such as bone formation (Kingsley *et al*., 1992). Executing their developmental programme, $\approx 10^5$ *Myxococcus* cells move into an aggregation centre, where they continue to move as they build a fruiting body. Within a nascent fruiting body, rod-shaped cells finally differentiate into spheroidal, environmentally resistant, non-motile myxospores.

Within any large field of developing cells, many fruiting bodies form, while some cells remain outside the organized structures. Those cells around and between fruiting bodies never sporulate; only cells within the nascent fruiting body become spores (O'Connor and Zusman, 1991; Julien *et al*., 2000). The peripheral cells express early developmentally regulated genes (Julien *et al*., 2000). This restriction of sporulation to the fruiting body structure ensures that each spore has the possibility of being transported as part of a macroscopic package. It also means that aggregation normally precedes sporulation. Evidently, spore transport is the function of a fruiting body (Bonner, 1982; Kaiser, 1999).

This spatial restriction of sporulation is a consequence of the different opportunities for signalling between cells (Julien *et al*., 2000). Of the five cell-to-cell signals used by *M. xanthus* during their fruiting body development (Hagen *et al*., 1978; Kaiser and Kroos, 1993), the C-signal plays a unique role in the spatial restriction of sporulation. The C-signal, a cell surface-associated protein coded by the *csgA* gene (Kim and Kaiser, 1990a; Shimkets and Rafiee, 1990), is required for both aggregation and sporulation (Shimkets *et al*., 1983; Søgaard-Andersen and Kaiser, 1996). The C-signal response pathway branches, with one segment controlling aggregative cell behaviour (Jelsbak and Søgaard-Andersen, 2000) and the other differentiation of spores (Søgaard-Andersen *et al*., 1996). In this paper, we investigate how the same signal leads to the differential timing of aggregation and sporulation. One key is that the intensity of C-signalling increases with time.

This investigation began with a mutant that retained the ability to construct mounded aggregates but made $< 10^{-6}$ the wild-type number of viable spores (Gorski *et al*., 2000). Significantly, the mutant produced much less C-signal than normal, as measured by either a sporulation rescue bioassay or the total amount of CsgA protein detected with specific antibody (Gorski *et al*., 2000). Here, we report the DNA sequence around the original mutant locus. That sequence revealed a cluster of four co-expressed genes, all of which regulate production of

Accepted 2 March, 2001. *For correspondence. E-mail Luttman @cmgm.stanford.edu; Tel. (+1) 650 723 6165; Fax (+1) 650 725 7739.

the C-signal. Two genes regulate the level and two the time of C-signal production. The activities of those genes show how fruiting body morphogenesis is regulated.

Results

The time course of C-signalling

C-signal, the product of the *csg*A gene, is necessary to form a fruiting body and to sporulate (Kim and Kaiser, 1990a; Søgaard-Andersen *et al*., 1996; Jelsbak and Søgaard-Andersen, 1999). The developmental time course of CsgA protein production is shown in Fig. 1. For this experiment, proteins extracted from a population of developing cells by boiling in SDS were electrophoretically separated in an SDS–polyacrylamide gel, then reacted with antibodies specific to the CsgA protein that had been generated by Kruse *et al*. (2001). The relative amount of CsgA protein was measured by the amount of antibody bound, control experiments having shown that bound antibody was proportional to the amount of CsgA protein (*Experimental procedures*). Also plotted in Fig. 1 are results of a C-factor bioassay, based on the ability of extracts of developing wild-type cells to rescue the sporulation of *csg*A mutant cells (Kim and Kaiser, 1990a). The Western and bioassay data agree within experimental error.

The amount of CsgA protein and signalling activity rise continuously and together to reach a maximum around 18 h. This time course spans the major morphological events in fruiting body development. Dashed lines at the top of Fig. 1 show the time periods over which three different C-signal-dependent processes – rippling, aggregation and sporulation – are observed. None of these occurs in *csgA*-deficient mutants (Li *et al*., 1992; Søgaard-Andersen *et al*., 1996). It is evident from Fig. 1 that the three are correlated with low, medium and high levels of CsgA activity. When these correlations are considered in the light of other experiments (Kim and Kaiser, 1991; Li *et al*., 1992), they imply that the expression of rippling, aggregation and sporulation genes has different threshold requirements for the intensity of C-signal. These data support the idea that the normal developmental progression from starvation to rippling to aggregation to sporulation results from the rise in CsgA activity shown in Fig. 1.

The act *operon*

The experiments described below show that the rise in CsgA activity depends on the *act* operon. The open reading frames (ORFs) in the DNA sequence upstream (pLAG66) and downstream (pLAG121) of the previously identified *act*1 gene (Gorski *et al*., 2000) are presented in Fig. 2. That sequence reveals a cluster of four adjacent ORFs that are oriented in the same direction, which will be called *act*A, *act*B, *act*C and *act*D. In view of their map location and the functional relations between these four genes, the name of the *act*1 gene has now been changed to *act*B.

Examination of the sequence to the left of *act*A revealed no ORFs on either strand within about 1000 bp. Moreover, a transcription start site was identified immediately to the left of *act*A with the aid of the primer, PE1, shown in Fig. 2. Messenger RNA was isolated by two different methods at 24 h of development, one using hot phenol and the other Qiagen reagents. A transcription start 57 bp ahead of the AUG of *act*A is defined by primer extension and illustrated in Fig. 3. The same start was found in both preparations, but only the Qiagen RNA is shown. The 24 h developmental RNA was fractionated by gel electrophoresis, and a 7.3 kb transcript was identified (Fig. 4). The RNA hybridizes to gene-specific probes for both *act*A (shown in the left lane of Fig. 4) and *act*D (shown in the right lane of Fig. 4). In another experiment, the amount of RNA that could hybridize to *act*A DNA and the amount that could hybridize to *act*B DNA was measured during development. Hybridization intensity changed with time in the same way for these two genes (data not shown). Thus, the four genes appear to be co-expressed and to constitute an operon whose left end is defined by the transcription start shown in Fig. 2. Investigation of the region beyond *act*D is planned; this report is focused on *act*A, *act*B, *act*C and *act*D.

Function of the act *operon products*

*act*A is predicted to encode a compound response regulator protein of 342 amino acids. Its amino end is similar to *che*Y protein, including an aspartate residue at the site in *che*Y at which it becomes phosphorylated (*che*Y Asp-57; Stock *et al*., 1985). The remainder of *act*A is similar to the putative output domains of two recognized response regulators: *ple*D of *Caulobacter crescentus* and its relative *cel*R2 of *Rhizobium leguminosarum* (Aldridge and Jenal, 1999; Ausmees *et al*., 1999). A figure showing these comparisons is available on this journal's web site (http://www.blackwell-science.com/mmi). The C-terminal domain of *ple*D has been shown to be essential for signal transduction in the polar morphogenesis of *C. crescentus* (Sommer and Newton, 1989; Aldridge and Jenal, 1999).

*act*B is predicted to encode a sigma-54 activator protein of 553 amino acids belonging to the NTRC family. It has an aspartate residue in its N-terminal region where NTRC is modified by phosphorylation, a highly conserved central region of several hundred amino acids containing an ATP-binding motif and a C-terminal region that contains a helix–turn–helix motif near its end (Gorski *et al*., 2000). *act*C is a multidomain protein of 437 amino

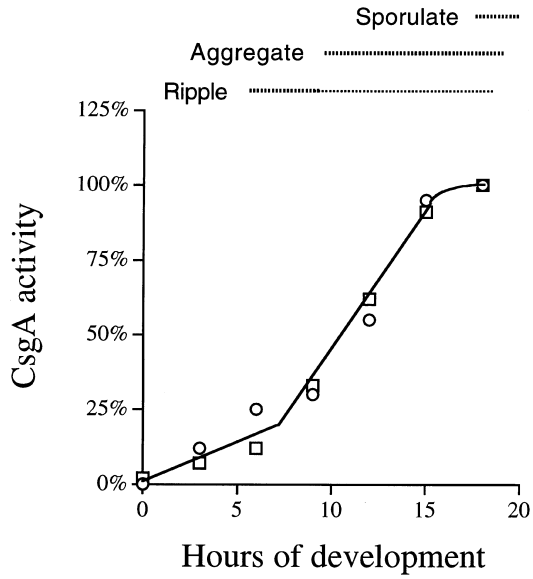

Fig. 1. Rise in C-signalling activity during development. Specific C-signal activity was measured on extracts of 5×10^7 cells developing in submerged culture. Activity was quantified by reaction with an antibody specific to the CsgA protein that had been produced by Kruse *et al*. (2001). The intensity of chemiluminescence, indicated by the open squares, was shown to be proportional to the amount of CsgA protein (*Experimental procedures*). Also plotted for comparison, as open circles, are data from Kim and Kaiser (1990a) of C-factor activity measured by the rescue of sporulation from a *csg*A-deficient mutant by partially purified extracts made at each time point. Shown above the graph by dotted lines are the periods of rippling (which decreases in the thinner part), aggregation and the start of sporulation in the wild type.

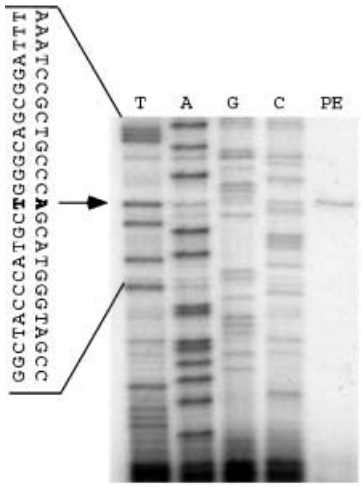

Fig. 3. Location of the transcription start site by primer extension. A primer (PE1 in Fig. 2) located about 70 bases downstream of the start was hybridized with the test RNA and extended using reverse transcriptase to produce cDNA complementary to the RNA template. DNA ladders for each of the four nucleotides were produced with a DNA template. The cDNAs were separated by electrophoresis, and their images are shown. The mRNA used as template is shown in the rightmost lane, headed PE. The initiating nucleotide and the sequence around it are shown to the left.

acids. Residues 275–411 resemble members of a family of N-acetyltransferases (NCBI Pfam 00583) that includes *rimI* of *Escherichia coli*. *act*D, predicted to encode a protein with 619 residues, appears to be a pioneer with no compelling relatives in the current GenBank database. The functions of all four *act* proteins are shown by the mutant studies described next.

Null mutations in act *A,* act *B,* act *C and* act *D.* An insertion mutant of *act*B (formerly *act*1) is unable to sporulate, although it does build mounds (Gorski *et al*., 2000). However, this insertion mutation is likely to be polar and, if so, the insertion strain might have the phenotype of an *act*B, *act*C, *act*D triple mutant. To identify the separate function of each of these four co-expressed genes, in frame deletion mutations were constructed in *act*A, *act*B, *act*C and an insertion mutation created in *act*D. The segments deleted in pTG019 ΔactA, pTG013 ΔactB, pTG015 ΔactC are indicated in Fig. 2. The figure also shows the segment cloned in pTG001; that plasmid was then inserted by homologous recombination into the site in *act*D marked Ωorf4. Additional details of these constructions are given in *Experimental procedures* and in Table 1. In constructing each deletion, care was taken to preserve the reading frame in the *act*A, *act*B and *act*C

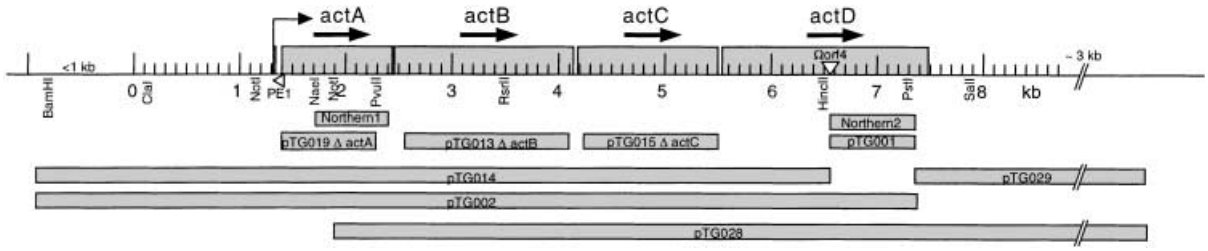

Fig. 2. Physical and genetic map of the *act* genes. Four open reading frames, *act*A, *act*B, *act*C and *act*D, oriented in the same direction are shown to scale. The DNA sequence was determined from pLAG66, pLAG121 and pTG030 (Table 3). Restriction sites are shown below the line. The primer used to locate the transcription start site is shown as a triangle labelled PE1, and its sequence is given in *Experimental procedures*. *act*A and *act*D probes for Northern blots are shown as Northern1 and Northern2. DNA segments that are deleted from pTG019 ΔactA, pTG013 ΔactB and pTG015 ΔactC are indicated by grey bars. The segments cloned in pTG001, pTG002, pTG014, pTG028 and pTG029 are indicated by their grey bars.

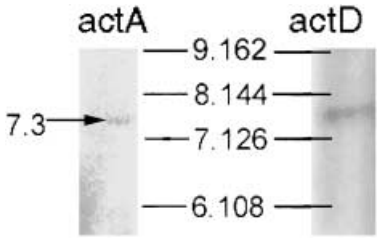

Fig. 4. A 7.3 kb RNA transcript of the *act* operon includes *act*A and *act*D. RNA isolated at 24 h from developing cells was separated by electrophoresis in a 1% agarose gel under denaturing conditions. The same gel was probed with either *act*A, shown on the left, or *act*D, shown on the right. RNA size markers, in kilobases, are shown in the centre.

genes to avoid polar effects. As a transcription stop has not yet been identified in the operon, the pTG001 insertion in *act*D may have a polar effect on any genes that lie beyond *act*D, to the extent that such genes are co-expressed with *act*D.

Aggregation. The same number of mutant and wild-type cells were plated on starvation medium (TPM), and their video images were recorded, starting at 9 h and extending to 2 days of development. Referring to the top row in Fig. 5, the wild-type standard for these developmental conditions and the parent of the *act* mutants begins to aggregate by 9 h. Wild-type aggregates become larger and rounder by 12 h; by 24–30 h, they have matured and, thereafter, show no further changes in size or shape. At the other extreme, a *csg*A null mutant, which is shown in the bottom row of Fig. 5, fails to form aggregates at any time. Although the field of *csg*A null cells is not completely formless, it illustrates the dependence of mounded aggregate formation on C-signalling. As to the *act* mutants shown in Fig. 5, the Δ*act*A, Δ*act*B and polar Ω*act*B mutants delay aggregation to ≈ 3 h later than the wild type. Although the delayed aggregation of Δ*act*B was reproducible, the Ω;*act*B sometimes failed to aggregate at all, as if a polar effect was inactivating one or more downstream genes as well as *act*B. The Ω*act*D mutant is even more delayed in aggregation than Δ*act*A or Δ*act*B; it aggregates about 12 h later than the wild type. In contrast, the Δ*act*C mutant begins to aggregate several hours earlier than wild type, forming aggregates that are slightly smaller than the wild type at every stage. Thus, mutants defective in *act*A, *act*B, *act*C or *act*D are able to form symmetrically mounded aggregates, but to a time schedule that is either retarded or advanced relative to wild type.

Rippling. In the wild type, rippling is evident during the first few hours of development, and it often accompanies the early stages of aggregation (Shimkets and Kaiser, 1982). Ripples are ridge-shaped heaps of cells, often seen in parallel ranks that travel across a field at constant speed (Sager and Kaiser, 1994). Rippling is completely dependent on C-signalling (Shimkets and Kaiser, 1982; Sager and Kaiser, 1994). As shown in Table 1, ripples are transient in the wild type (DK1622); they are present in every aggregation field before 21 h but, by 24 h, they are absent in most fields and, by 36 h, none of 100 wild-type fields had ripples. Their transience is a consequence of aggregation, because most cells move into one or other mounded aggregates leaving few cells between the aggregates to build ripple heaps. In striking contrast to the wild type, the data in Table 1 show that the Δ*act*A and Δ*act*B aggregation fields are more than 50% covered with ripples at 24 h; at 48 h, 86% of fields have more than 1% of their area covered with ripples, and 10–20% of fields are still rippling at 96 h. Although rippling is common in the Δ*act*A and Δ*act*B mutants at late developmental times, it is infrequent in the wild type or in the *act*C or *act*D mutants at later times (Fig. 5). Several complete developmental time courses were monitored in addition to the experiment in Fig. 5, and no late ripples were seen in any of the wild-type, *act*C or *act*D mutant sequences.

Persistence of ripples in the Δ*act*A and Δ*act*B mutant cultures has two implications. It implies that C-signalling conditions appropriate for rippling persist. It also implies that the density of cells remaining outside the aggregates is greater than in the wild type at the same time. As the numbers of aggregates are about the same for wild-type and the *act* mutants (Fig. 5, at 48 h), it also follows that

Table 1. Frequency of rippling as a function of developmental time in wild-type, *act*A and *act*B strains.

DK1622 cultures with ripples Fraction of spot	12–21 h	22 h	23 h	24 h	36 h
0%	0	0	12	83	100
< 5%	0	0	74	9	0
5–20%	0	1	9	4	0
20–50%	0	28	3	3	0
> 50%	100	72	2	1	0

Mutant cultures with ripples	24 h		48 h		72 h		96 h	
Fraction of spot	*act*A	*act*B	*act*A	*act*B	*act*A	*act*B	*act*A	*act*B
0%			4	8	24	29	88	80
< 5%			44	33	56	43	9	18
5–20%			20	25	16	21	3	2
20–50%			16	17	4	7	0	0
> 50%	100	100	16	17	0	0	0	0

One hundred spot cultures of each strain on starvation agar plates were screened for the presence of ripples at the times indicated. The fractional area of each spot covered by ripples was measured, expressed as a percentage, and those data placed into one of the six classes listed. 0% indicates no ripples in any culture. < 5% indicates the number of cultures with ripples that occupied less than 5% of the culture area.

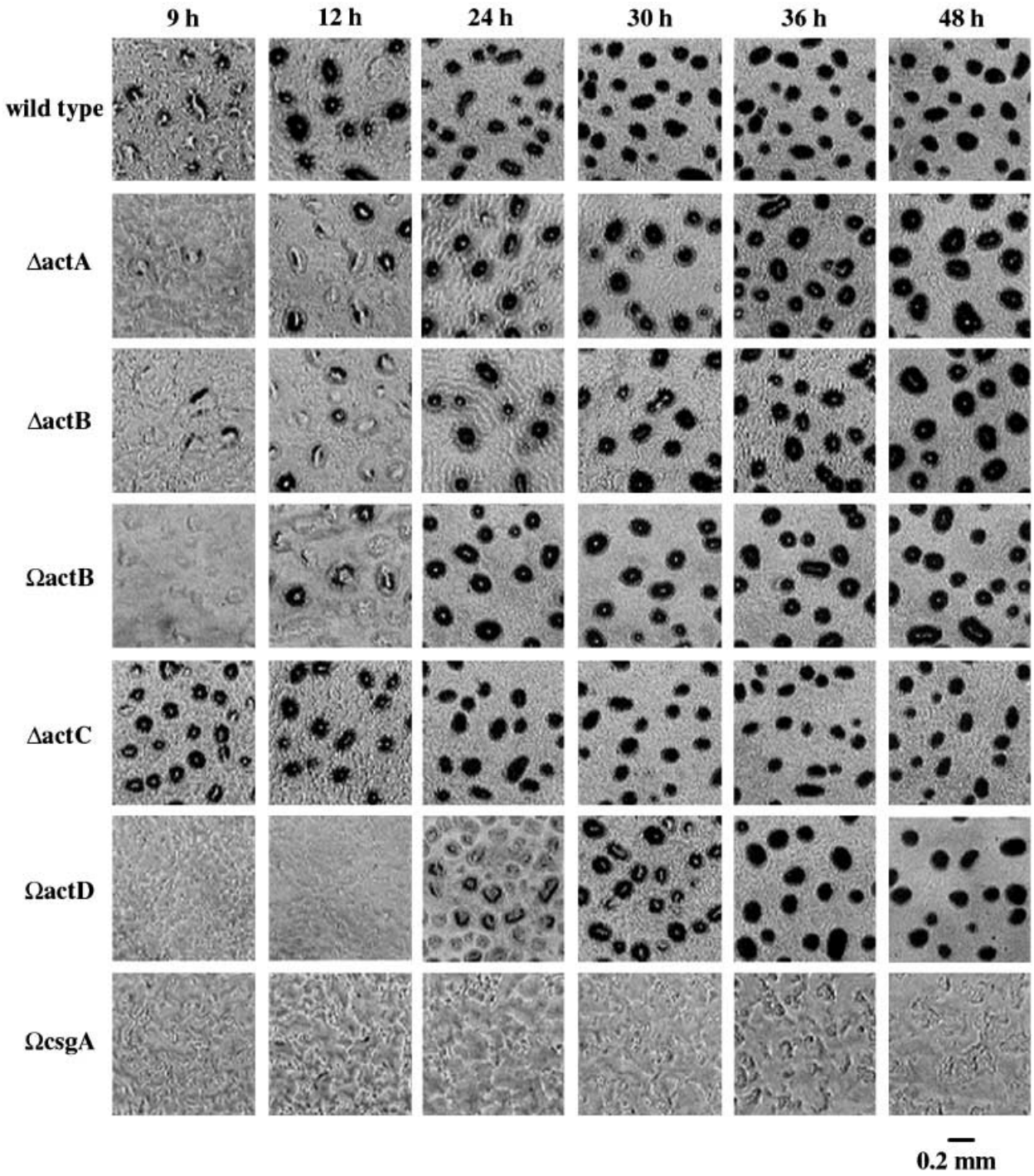

Fig. 5. Aggregation of *act* mutants compared with wild type (DK1622) and a *csg*A mutant. Videographs of sample microscopic fields were taken at 9 h to 48 h of cultures developing on starvation agar (TPM). Culture plates were incubated at 32°C, removed, examined at room temperature with phase-contrast optics at the time indicated, then returned to 32°C. Each image is thus a different microscopic field and a different sample of the whole culture. Fruiting bodies are evident as circular or elliptical, darkened mounds in the wild type from 9 h onwards. Ripples are evident in the 12 h image of the wild type and the 24 h images of the *act*A and *act*B strains.

there are somewhat fewer cells within the Δ*act*A and Δ*act*B mutant aggregates than in the wild type. Microscopic examination of these Δ*act* aggregates shows that they have about the same diameter as the wild type, but have lower altitudes and thus fewer cells. More evidence for fewer cells in these aggregates compared with wild type is that the Δ*act*A, Δ*act*B and *act*B mutant aggregates have a white dot in their

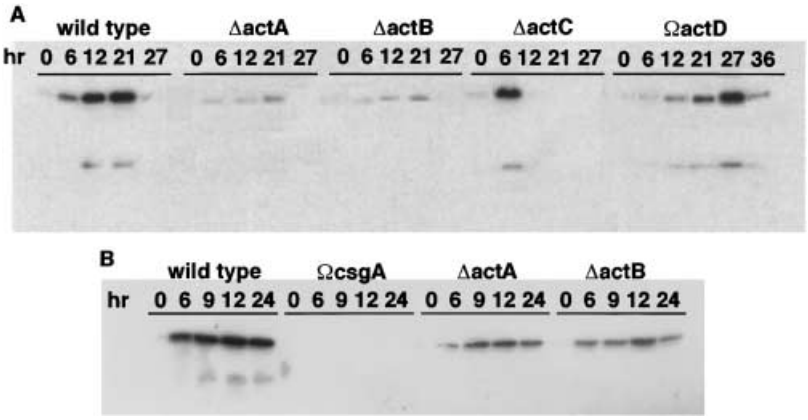

Fig. 6. Western blots of CsgA protein sampled at various times of development. SDS–polyacrylamide gels were exposed to specific CsgA protein antibody (Kruse *et al.*, 2001). Cells developing in submerged culture in plastic wells were harvested at the developmental time indicated (hours), thus providing the same total mass of cells for each sample. Protein from $\approx 5 \times 10^7$ cells was analysed for each electrophoresis lane. The amount of CsgA protein in each band was measured by its chemiluminescence.
A. Wild type (DK1622) and *act* mutants.
B. Wild type (DK1622), a null *csg*A mutant, *act*A deletion and *act*B deletion.
A longer exposure was made for (B) than for (A) to visualize better the residual amount of CsgA protein in the *act*A and *act*B deletion mutants.

centres at 48 h in Fig. 5, whereas the wild type has a white dot only up to 24 h. Several Δ*act*B aggregates were opened, revealing cells that had a variety of ovoid shapes. Evidently, these cells are viable because, when such aggregates were transferred on a filter disk from starvation to a nutrient-rich agar (CTT), rod-shaped cells emerged, swarmed outwards and grew like cells before starvation.

Sporulation. The number of viable spores was measured from 1 to 7 days after the induction of development by starvation (Table 2). For comparison, from 5×10^8 cells initially plated, the wild type produced 1.1×10^6 heat- and sonication-resistant spores. No viable spores were detected in any experiment with the Δ*act*A and Δ*act*B mutants, which implies $< 10^{-6}$ of wild-type sporulation and an amount similar to the *csg*A mutant DK5208 (Table 2). Evidently, both *act*A and *act*B genes are required for sporulation. The *act*C mutants that begin to aggregate earlier than wild type (Fig. 5) also begin to sporulate earlier: a significant number of spores were detected in this experiment on day 1, but not until day 2 in the case of wild type. However, after the first day, the *act*C mutant never formed more than half the number of wild-type spores, and final sporulation was 19% of wild type. The *act*D mutant that delayed aggregation never had more than 18% of the number of wild-type spores. All four *act* genes play important roles in sporulation: *act*A and *act*B are crucial, whereas *act*C and *act*D are needed for full sporulation efficiency.

Table 2. Sporulation.

	Number of spores					
Day	Wild type	*act*A	*act*B	*act*C	*act*D	*csg*A
1	0, 0	0	0	150, 260	0	0
2	2.5×10^5	0	0	1.2×10^5	2.9×10^4	0
3	6.2×10^5	0	0	1.6×10^5	8.7×10^4	0
5	1.0×10^6	0	0	2.0×10^5	1.7×10^5	0
7	1.1×10^6	0	0	2.1×10^5	2.0×10^5	0

The number of viable, heat- and sonication-resistant spores arising from 5×10^8 cells initially added in five droplets on the surface of a starvation agar plate were counted, as described in *Experimental procedures*. Droplets were harvested after 1, 2, 3, 5 and 7 days at 32°C. Counts for two independent experiments are shown after 1 day for wild type and *act*C.

The act *genes control the timing and level of* csg*A expression*

The Western blot in Fig. 6A shows the time course of CsgA protein production for wild type (DK1622) and for mutants in each gene of the *act* operon. Another experiment with a longer exposure is shown in Fig. 6B. It includes a *csg*A mutant (DK5208), which produces no biologically active CsgA protein, and confirms the specificity of the antibody. The blot shows that the Δ*act*A and Δ*act*B mutants produce a low level of C-signal. At each time point, the mutants had no more than one-quarter of the level of the wild type. Additional experiments were performed to find the time of maximum CsgA protein production in each mutant within an hour, and Fig. 6 portrays the optimized protocol. The DK1622, Δ*act*A, Δ*act*B comparisons have been repeated three times with very similar results. Evidently, the Δ*act*A and Δ*act*B mutants produce enough C-factor to induce rippling (Table 1) and aggregation (Fig. 5), but not enough to trigger sporulation (Table 2).

The *act*C and *act*D null mutants produce at least 95% as much CsgA protein as the wild type, as indicated by the comparable degrees of maximum darkening in Fig. 6. However, their time course is very different; the *act*C mutant reaches its maximum at 6 h, about 15 h earlier than the wild type. In contrast, the *act*D mutant reaches its maximum at 27 h rather than the 21 h in the wild type, delaying maximum C-factor production by about 6 h. It should be emphasized that these measurements of CsgA levels were made at the same time on a parallel set of

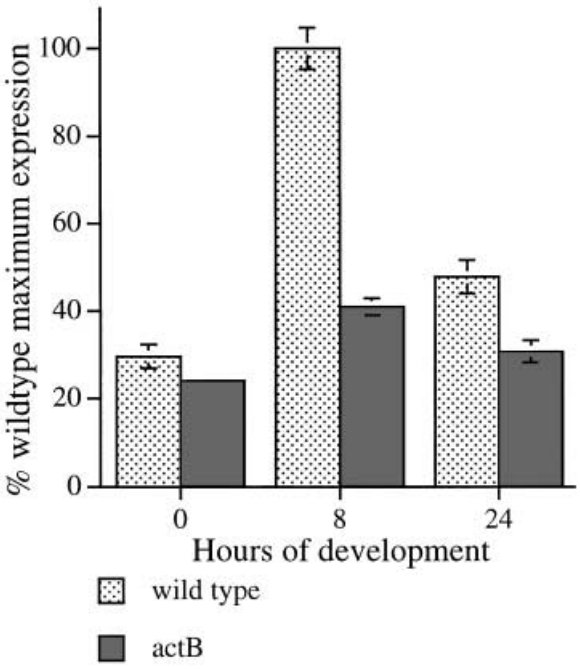

Fig. 7. Transcription of the *csg*A gene. The amount of *csg*A mRNA was measured by hybridization after 0, 8 and 24 h of development in wild-type and *act*B mutant cells. The *csg*A hybridization probe DNA was derived from pLJS43 (Table 3).

cultures, with the same number of cells harvested from each well of the plastic culture plate, to facilitate direct comparison of the levels in several cultures.

The act *operon controls the level of* csg*A mRNA*

RNA was isolated from developing wild-type and *act*B mutant cells at 0, 8 and 24 h after starvation had induced development. *csg*A mRNA was measured by hybridization to an internal fragment of the gene. Hybridization intensity data are presented in Fig. 7. In agreement with the measurements of CsgA protein by Western blotting in Fig. 6, the message level in the wild type (DK1622) was low at 0 h and higher at 8 h. At 24 h, this has fallen from the 8 h peak just as the CsgA protein at 27 h has fallen from its 21 h level. The Δ*act*B mutant mRNA levels also agree with the observed lowering of CsgA protein levels in that mutant. All six data points in Fig. 7 show agreement between relative levels of mRNA and relative levels of protein. This agreement implies that CsgA protein levels are primarily governed by *csg*A mRNA levels, which are regulated in turn by the *act* operon.

Discussion

Four *act* genes are co-transcribed from a single start 57 bp upstream of *act*A. A 7.3 kb RNA transcript has been detected that hybridizes to *act*A and *act*D. Both the size of this transcript, which would extend from the start right through *act*D, and the fact that it includes *act*A and *act*D sequences argue that the four genes are co-transcribed on the same messenger RNA. As an operon, the function of the *act* genes is to control the level and time of *csg*A expression.

Individually, the *act*A and *act*B genes are seen to control the level of CsgA protein (Fig. 6). The *act*A and *act*B mutants do not affect the rise and fall of CsgA expression in time, only its maximum level. The *act*B mutant is shown to produce less *csgA* mRNA (Fig. 7), suggesting that *act*A and *act*B are specialized transcriptional regulators, in agreement with the sequence similarity of *act*B to NTRC. The *act*A and *act*B deletion mutants produce one-quarter as much CsgA protein as the wild type and are unable to sporulate even though they can aggregate. The failure to sporulate clearly reflects the higher CsgA threshold for sporulation than for aggregation. Remarkably, the functions of *act*C and *act*D are also implied by the measurements of CsgA levels, as they contrast with wild type, Δ*act*A and Δ*act*B. Although the *act*C and *act*D null mutants produce as much CsgA protein as wild type, their time course is different. The *act*C mutant reaches its maximum 15 h earlier than wild type, whereas the *act*D mutant delays maximum C-factor production by about 6 h. Thus, it appears that the normal ActC protein actually delays, whereas the normal ActD advances *csg*A expression. As a consequence of these defects in timing of CsgA protein production, aggregation is premature in the *act*C mutant and delayed in the *act*D mutant. These timing differences without level differences also reduce sporulation significantly. Apparently, both *act*C and *act*D proteins are needed to achieve the optimal timing of CsgA expression in order to maximize sporulation.

The fact that at least four *act* proteins and perhaps as much as 1 kb of *csg*A upstream DNA (Li *et al*., 1992) are devoted to controlling the timing and level of expression of *csg*A reflects the central role that CsgA protein plays in orchestrating aggregation and sporulation. Those elements may have been selected to optimize the number of spores within a fruiting body. Considering that sporulation is a response to starvation and assuming that the function of a fruiting body is to assemble spores into a macroscopic package that facilitates spore transport by a passing animal to a new place where nutrients are likely to be available (Bonner, 1982; Kaiser, 1999), such selection would be expected.

The product of the first gene, *act*A, is similar to the compound response regulators, *ple*D of *C. crescentus* and *cel*R2 of *R. leguminosarum*. The similarity includes a complete *che*Y sequence with an aspartate at the site that becomes phosphorylated in CheY protein during chemotaxis. These are followed in *act*A by a truncated *ple*D

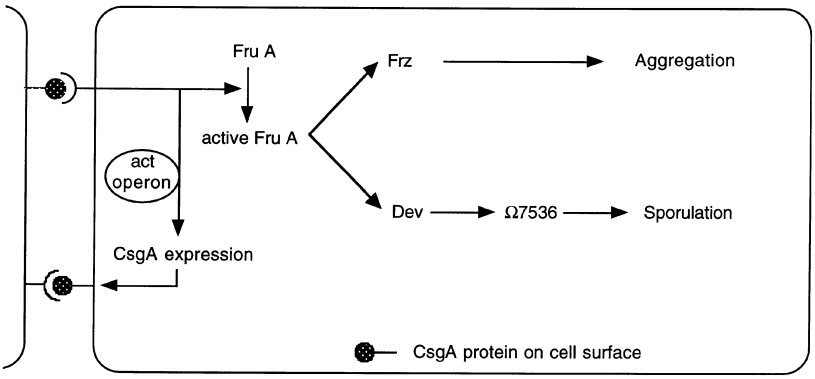

Fig. 8. The C-signal transduction pathway modified from Julien *et al.* (2000). Two cells are shown signalling to each other. Both cells have the same transduction circuit but, for clarity, it is shown only in the cell on the right. C-factor has been identified adhering to the surface of cells (Shimkets and Rafiee, 1990); its sensor has not yet been identified. The pathway is based on Ogawa *et al.* (1996), Søgaard-Andersen *et al.* (1996), Ellehauge *et al.* (1998) and Licking *et al.* (2000). The positive feedback step regulated by *act*A, B, C and D is shown.

C-terminal domain, which has been shown to be required for *ple*D function in signal transduction (Aldridge and Jenal, 1999). ActB is a transcriptional activator protein of the sigma-54 class (Gorski *et al.*, 2000). If *act*A is a response regulator, then the facts that *act*A and *act*B are adjacent and that their deletion mutants have the same aggregation and sporulation phenotypes suggest that the *act*A and *act*B gene products are part of the same signal transduction pathway, one that governs *csg*A expression.

*act*B encodes a transcriptional activator protein that strongly resembles NTRC (Gorski *et al.*, 2000). NTRC is known to bind enhancer sequences (Wedel *et al.*, 1990), and it is possible that *act*B finds an enhancer in the *csg*A regulatory region. Although a sigma-54 promoter has not been identified there, direct action by *act*B is suggested by the fact that the four *act* null mutants bring about relatively large changes in timing and level of CsgA protein, seldom seen when action is indirect. Moreover, an NTRC-like protein in *Rhodobacter capsulatus* has been shown to activate the transcription of several genes that are not sigma-54 dependent (Foster-Hartnett and Kranz, 1994; Foster-Hartnett *et al.*, 1994), providing a precedent. Whether by direct or indirect action, we propose that the output of an *act*A *act*B signal transduction pathway regulates the expression of *csg*A. We also suggest from the ensemble of data presented here that the sensory input to this putative *act*A *act*B transduction pathway is the transmission of the C-signal. If true, a positive feedback loop would be created that would cause the intensity of C-signalling to rise progressively as development proceeds up to the time of sporulation. Such a rise is documented in both experiments in Fig. 1.

This rising level of CsgA appropriately induces the expression of individual C-signal-dependent aggregation genes and spore initiation genes, which have different C-signalling thresholds (Kim and Kaiser, 1991; Li *et al.*, 1992). These genes are expressed in order: first aggregation, then sporulation. Kim and Kaiser (1991) showed that *csg*A null cells require a certain threshold level of partially purified C-factor to activate expression of the 4 h aggregation reporter, Ω4499, and a distinctly higher level for the sporulation reporter Ω4435. Li *et al.* (1992) proposed a similar ranking of required CsgA levels, based on a correlation between the extent of deletion of the *csg*A promoter region and the extent of development. Recently, Kruse *et al.* (2001) have constructed CsgA under- and overproducing strains with one or many copies of the *csg*A gene that independently support the ordered thresholds and the effects of different CsgA levels on development that are described here.

How the rise in C-signal accounts for the succession of aggregation and sporulation follows from the C-signal response pathway of Fig. 8. That pathway is based on the whole body of published work on C-signalling, to which the *act*-dependent positive feedback loop has been added. The developmental process starts with CsgA protein found on the cell surface (Shimkets and Rafiee, 1990), which is represented by lollipops in Fig. 8. CsgA protein transmits the C-signal by cell-to-cell contact (Kim and Kaiser, 1990b). Although the molecular mechanism of transmission remains to be clarified, the transmission of C-signal enhances *csg*A expression as described above. After initial episodes of C-signalling, an increase in the amount of CsgA protein per cell is observed (Kim and Kaiser, 1991; Gorski *et al.*, 2000; Fig. 1 in this paper). When a cell that carries elevated C-signal transmits that signal to another cell, the amount of activated FruA rises in the latter until it reaches the aggregation threshold. At that threshold, FruA would activate the *frz* phosphorelay on the upper branch of Fig. 8 (Søgaard-Andersen and Kaiser, 1996; Ellehauge *et al.*, 1998; Kruse *et al.*, 2001). The *frz* phosphorelay modulates cell movement parameters (Blackhart and Zusman, 1985). At this threshold, the C-signal-induced changes are to increase cell speed and to decrease the stop and reversal frequencies (Jelsbak and Søgaard-Andersen, 1999). Cells whose behaviour is changed in this way form chains that stream into the mounds and increase their volume (Jelsbak and Søgaard-Andersen, 1999; 2000). Such multicellular streams are vividly portrayed in the time-lapse recorded films of H. Reichenbach (Kuhlwein and Reichenbach,

1968). The cells continue to stream within a mound, apparently moving in closed orbits and giving the mounds their observed circular symmetry (O'Connor and Zusman, 1989; Sager and Kaiser, 1993; White, 1993). Such mounds are observed to pulsate (Kuhlwein and Reichenbach, 1968), which might be a consequence of cyclic cell movement inside. As the cells stream at high density within a mound, they would frequently collide end-to-end like logs in a stream. More C-signalling and positive feedback would follow. The CsgA level on cells within a mound would thus climb continuously upwards. Eventually, the signal intensity would reach the sporulation threshold. The final set of genes that differentiate spores would produce their products, some of which may have been identified (Licking *et al*., 2000).

This progression from aggregation to sporulation would be interrupted by null mutations in the *act*A or *act*B genes, which limit the transcription of *csg*A. CsgA protein levels rise in these mutants but, as shown in Fig. 6, they never rise above one-quarter of those of DK1622. Although this level may be sufficient to induce aggregation, it may not do so completely or in all cells. The average aggregate formed by *act*A and *act*B mutants has fewer cells than DK1622, and the cell masses have lower altitudes. Ripples are evident as late as 96 h (Table 3) in these mutants, because the lower CsgA levels observed in *act*A and *act*B mutants are comparable with levels in the early, rippling phase of DK1622. In addition, more cells remain unaggregated; cells remaining outside aggregates can build the ridges of ripples. An important consequence of the lower peak CsgA levels in the *act*A and *act*B mutants is that sporulation is never induced. These mutants form only 10^{-6} of the number of spores as DK1622, a number comparable to *csg*A null mutants, as the circuit of Fig. 8 would predict. In contrast, *act*C and *act*D null mutants, which synthesize as much CsgA protein as DK1622, not only aggregate, but also sporulate. They form somewhat fewer spores than DK1622, perhaps because C-signal peaks too early in an *act*C mutant or too late in *act*D. Nor do *act*C and *act*D mutants prolong rippling; once their aggregation begins, it progresses further than *act*A and *act*B mutants because of higher CsgA levels.

Careful examination of the Western blots in Fig. 6 reveals two protein bands reacting with the Kruse *et al*. (2001) CsgA specific antibody: a strong, upper band migrating as a protein of about 25 kDa and a lower, weaker band at about 17 kDa. These two sizes probably correspond, respectively, to a full-length *csgA* product (Lee *et al*., 1995) and the C-factor active *in vitro* in the sporulation rescue assay (Kim and Kaiser, 1990c). Peptide sequencing showed that the partially purified C-factor was encoded by the *csg*A gene (Kim and Kaiser, 1990a). Kruse *et al*. (2001) made the reasonable suggestion that the 17 kDa protein may arise by proteolytic processing of a primary 25 kDa translation product. This suggestion remains to be tested experimentally. The relative intensity of the two bands in Fig. 6 indicates that they are present at about the same mass ratio in DK1622 at several time points and in the four *act* mutants. Moreover, the fact that the two sets of experimental points in Fig. 1, which correspond to the two products of csgA, fit the same curve supports a constant ratio of 17 kDa bioactive C-factor to 25 kDa CsgA protein

Table 3. *M. xanthus* strains and plasmids.

Strain or plasmid	Relevant characteristics	Reference or source
M. xanthus		
DK1622	Wild type	Kaiser (1979)
DK5208	Tn5-132::*csg*A	Kroos and Kaiser (1987)
DK7837	pLAG2::*act*B	Gorski *et al*. (2000)
DK10601	pTG001::*act*D	This work
DK10603	Δ*act*B	This work
DK10604	Δ*act*C	This work
DK10605	Δ*act*A	This work
Plasmids		
pBGS18	Km^R	Spratt *et al*. (1986)
pBluescript	Amp^R, SK+	Stratagene
pBJ114	Km^R and galactokinase	Julien *et al*. (2000)
pLAG66	Cloned 3.7 kb *act* DNA fragment	Gorski *et al*. (2000)
pLAG121	Cloned 4.7 kb *act* DNA fragment	Gorski *et al*. (2000)
pLJS43	Complete *csg*A gene	Li *et al*. (1992)
pTG001	810 bp internal fragment of *act*D from pLAG 121 into pBGS18	
pTG002	8.5 kb fragment upstream of the pTG001 insertion in DK10601	
pTG013	In frame deletion, Δ*act*B	Table 4
pTG014	7.5 kb *Bam*HI–*Hin*cII fragment from pTG002 in pBJ114	
pTG015	In frame deletion Δ*act*C	Table 4
pTG019	In frame deletion Δ*act*A	Table 4
pTG028	pBGS18 with 11.5 kb *Not*I DNA fragment of *act*A and beyond *act*D	
pTG029	6.5 kb *Sal*I–*Not*I fragment of pTG028 inserted into pBluescript	

in DK1622 cells. As suggested in Fig. 1, the ratio remains constant as the C-signal rises from low levels early in development to high levels during sporulation.

Experimental procedures

Cultures

The *M. xanthus* strains and plasmids used are listed in Table 3. General procedures for growth and development have been described previously (Gorski *et al*., 2000). *M. xanthus* cultures were propagated at 32°C in CTT broth (1% bacto casitone, 10 mM Tris-HCl, pH 8.0, 8 mM $MgSO_4$, 1 mM KPO_4, pH 7.6) or CTT agar (CTT broth plus 1.5% bacto agar). Kanamycin (20 $\mu g\ ml^{-1}$ in CTT broth or 40 $\mu g\ ml^{-1}$ in CTT agar; or 5 $\mu g\ ml^{-1}$ gentamicin or 12.5 $\mu g\ ml^{-1}$ tetracycline) was added where indicated. TPM buffer (10 mM Tris-HCl, pH 7.6, 8 mM $MgSO_4$, 1 mM KPO_4, pH 7.6) and TPM agar (TPM buffer plus 1.5% bacto agar) were used to induce development as described previously (Kroos *et al*., 1986); exponential cells grown to a density of 5×10^8 cells ml^{-1} were harvested by centrifugation and resuspended in TPM buffer at a concentration of 5×10^9 cells ml^{-1}. Droplets (20 μl) were placed on the surfaces of TPM agar plates to measure fruiting body development. For cloning purposes, *E. coli* DH10B cultures were grown in L broth or L agar (Sambrook *et al*., 1989) supplemented with ampicillin or kanamycin (20 $\mu g\ ml^{-1}$ in L broth or 40 $\mu g\ ml^{-1}$ in L agar) where indicated.

Cloning the act *operon*

In situ cloning was used to isolate wild-type chromosomal DNA in the vicinity of *act*. DNA from DK10601 was restricted with *Bam*HI for DNA upstream of the *act* insertion in this strain, and an 8.5 kb fragment was used to create the plasmid pTG002. DNA from DK10601 was restricted with *Not*I, and an 11.5 kb fragment containing DNA upstream and downstream of the insertion was used to create the plasmid pTG028. For DNA downstream of the insertion, pTG028 was cut with *Pst*I and *Not*I, and a fragment was cloned into pBluescript SK+ cut with the same enzymes, creating pTG029. *E. coli* strain DH10B was transformed by electroporation with the ligation products for each plasmid, then plated onto Luria–Bertani (LB) agar with kanamycin. Plasmid DNA was isolated from the transformants and digested with the appropriate enzymes to confirm the structure of the plasmid clones. pTG002 contains $\approx$7.5 kb of DNA upstream of the pTG001 insertion. pTG029 contains $\approx$7 kb of DNA downstream of the same insertion. Plasmid manipulation and DNA isolation were performed as described previously (Sambrook *et al*., 1989).

Sequencing of DNA

Sequencing was carried out by standard methods at the Stanford University Protein and Nucleic Acid Facility and at Davis Sequencing. A combination of *Exo*III deletions and primer walking was used to sequence pLAG66, pLAG121 and pTG030. Sequence homology searches used several forms of the BLAST program from NCBI. These sequence data for the *act* operon have been submitted to GenBank under accession number AF350253.

Construction of in frame deletions

pTG014 (Table 3) contains 2 kb of *M. xanthus* DNA upstream of *act*A and 2 kb downstream of *act*C in the vector pBJ114, which includes the galactokinase gene for negative selection. In frame deletions of *act*A, *act*B and *act*C were constructed from pTG014, using the polymerase chain reaction (PCR) as follows. Pairs of primers were designed for reverse PCR on pTG014 as template; primer sequences are given in Table 4. The primers that hybridize to opposite strands are called Forward and Reverse. Each primer has an A_3C or G_3C tail, an *Xba*I or *Nde*I restriction site followed by a sequence homologous to the beginning or end of the gene. The restriction sites were engineered into the primers in order that the resulting PCR product could join its own ends to create the closed circular deletion plasmid. After PCR with the Expand Long Template PCR system (Roche), the template DNA was digested with *Dpn*I, which only cleaves methylated DNA. The PCR product was digested with *Xba*I or *Nde*I, which do not cut in pTG014 but only in the newly created ends of the PCR product. The cleaved sites at the two ends of the PCR product were allowed to join, then ligated, and the DNA was electroporated into DH10B. The plasmid was sequenced to confirm that the deletion was in frame. The plasmids pTG013, pTG015 and pTG019 were electroporated into DK1622. By selecting for kanamycin resistance carried by the plasmids, tandem duplication strains were recovered. Finally, the plasmid was allowed to loop out, removing with it one of the tandem copies of the gene. Mutant strains that had lost the plasmid became resistant to galactose and were selected by plating the cultures on CTT with 1% galactose. Those mutant strains, now Km^S, had either a wild-type or a deleted copy of the gene. The deletion mutant strains were confirmed by Southern blotting and, finally, by using them as templates for PCR synthesis.

Sporulation assay

The sporulation procedure of Gorski *et al*. (2000) was modified as follows. Five 20 μl spots containing 10^8 cells each were placed on TPM agar plates, allowed to develop at 32°C, and the cell mass was scraped off and suspended in TPM buffer. The cells and spores were treated in an ice-cooled Vibra Cells TM cup sonicator (Sonics Materials) for 3 min at amplitude 50 to disrupt fruiting bodies and disperse spores. Residual vegetative cells were subsequently killed by heating the tubes at 49°C for 2 h. The sporulation efficiency was measured as the number of colonies growing on CTT supplemented with the antibiotic appropriate to the strain being assayed (kanamycin, tetracycline or gentamicin) relative to the number of viable cells initially deposited on the TPM agar plates.

Table 4. In frame deletion primers.

Gene	*Restriction site* **Homologous region**	Distance to start or stop	Deletion size
*act*A, pTG019 *Nde*I			
Reverse AAAC*CATATG***CCCCATCCTGACTTCCTCAT**		3 bp	1008 bp
Forward AAAC*CATATG***CGGTTGTCGGTGTGAGGGTG**		12 bp	
*act*B, pTG013 *Xba*I			
Reverse GGGC*TCTAGA***CATCCCCTCGCCTCCACTCG**		0 bp	1656 bp
Forward GGGC*TCTAGA***TAGGTGAGCCGTAACCGTCG**		0 bp	
*act*C, pTG015 *Xba*I			
Reverse GGGC*TCTAGA***CGAGAGGAGGCGTCATGTCCC**		46 bp	1290 bp
Forward GGGC*TCTAGA***CCCTGTGAGCCGAGCCGGGTGACAG**		5 bp	

Forward and reverse primers were created for each of *act*A, *act*B and *act*C. Reverse *act*A, for example, indicates the primer complementary to the predicted sequence of *act*A DNA. It starts upstream of the *act*A deletion. Forward *act*A indicates the primer in the direction of the predicted 5′−3′ sequence. It starts downstream of the deletion. Each primer consists of an A_3C or G_3C tail, an *Nde*I or *Xba*I restriction site and a region homologous to the gene to be deleted. The pair of forward and reverse primers was used for PCR on pTG014 template DNA. The synthesized product was cut with the appropriate restriction enzyme to create a plasmid containing at least 2 kb of the sequence around the deletion as well as a restriction site. The distance between the translation start of the gene and the deleted region is shown for the reverse primer, and the distance between the deleted region and the translation stop site is shown for the forward primer. The size of the resulting deletion is shown.

Rippling

Five 20 μl spots containing 10^8 cells each were placed on TPM agar plates and allowed to develop at 32°C. The spots were examined microscopically with a 2.5× brightfield and a 6.3× phase-contrast objective. The images were measured relative to the lines of a Petroff–Hausser bacterial counter grid that provided the scale.

Western blotting

Standardized Western blot hybridization was used to monitor the level of CsgA protein with an anti-CsgA antibody (Kruse *et al*., 2001). Cells were allowed to develop in submerged culture in A50 buffer and harvested as described previously.

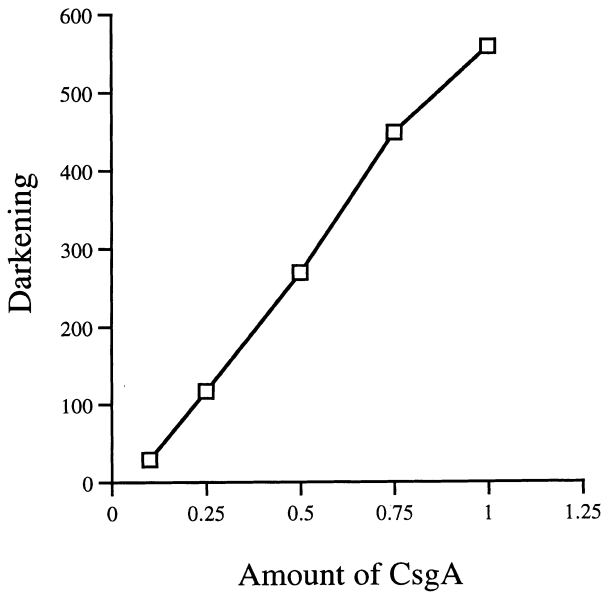

Fig. 9. Quantification of CsgA protein by Western blot. The indicated relative amounts of an extract of wild-type cells was electrophoresed in an SDS–polyacrylamide gel.

Cell pellets were resuspended in 50 μl of sodium dodecyl sulphate (SDS) sample buffer, and protein from ≈ 5 × 10^7 cells was analysed. Standard SDS–PAGE conditions (Sambrook *et al*., 1989) were used to reveal the CsgA protein. The secondary antibody was conjugated to horseradish peroxidase for chemiluminescence. The chemiluminescence is proportional to the amount of CsgA protein added (Fig. 9).

Developmental RNA

Approximately 1–2 × 10^{10} cells were spread on TPM plates, incubated at 32°C, then harvested into TPM buffer by scraping and pelleted by centrifugation. RNA was isolated according to the protocol of the RNeasy Midi Spin columns (Qiagen). The cells were disrupted by resuspending them in lysozyme-containing TE buffer, then treating them with ultrasound.

Quantification of RNA with a DNA probe

RNA samples (3 μg) were prepared with 25 μl of 2 mM EDTA, 30 μl of 20× SSC (Sambrook *et al*., 1989) and 20 μl of 37% formaldehyde in a total volume of 100 μl and heated at 60°C for 15 min. The samples were transferred to Hybond-N nylon membrane (Amersham) according to the protocol for the Bio-Dot SF (Bio-Rad) with 10× SSC and UV cross-linked to the membrane. The membranes were set up as a Southern blot with DNA samples as a probe that were ^{32}P-labelled using standard procedures (Sambrook *et al*., 1989).

Reverse transcriptase primer extension

A primer starting about 70 bases downstream of the presumed start, namely CCCCGGATTTACAGCCTCGAA CC, was labelled at 37°C using T4 polynucleotide kinase and 30 μCi of [γ-^{32}P]-dATP. The primer was purified with the Sephadex G-50 Quick Spin column (Boehringer), mixed with 40 μg of RNA from developing cells and used in a reverse transcriptase reaction as described previously (Wu and

Kaiser, 1997) to determine the transcriptional start site of the *act* operon. The same primer was used for double-stranded cycle sequencing according to the ThermoSequenase cycle sequencing kit (USB) to generate a DNA ladder for each of the four nucleotides. Standard PAGE conditions (Sambrook *et al*., 1989) were used to reveal the primer extension and the DNA ladder with Kodak scientific imaging film Biomax MR.

Northern blot

RNA (20 μg) was separated on a 1% agarose gel containing 2.2 M formaldehyde and blotted onto a Hybond-XL nylon membrane. DNA probes for *act* A and *act* D, shown in Fig. 2, were labelled with ^{32}P and used to hybridize to the RNA to reveal the size of the RNA bands containing *act* A and *act* D.

Supplementary material

The following material is available from http://www.blackwell-science.com/products/journals/suppmat/mmi/mmi2428/mmi2428sm.htm

Figure S1 Sequence alignments of a conceptual translation of Act A with *E. coli che Y* (upper three rows; the lower five show Act A starting with its residue 61 and extending to its C-terminus).

Acknowledgements

The antiserum to CsgA was a kind gift from T. Kruse, S. Lobendanz, N. Berthelsen and L. Søgaard-Andersen, Odense University. This investigation was supported by US Public Health Service grant GM 23441 to D.K. from the National Institute of General Medical Sciences.

References

Aldridge, P., and Jenal, U. (1999) Cell cycle-dependent degradation of a flagellar motor component requires a novel-type response regulator. *Mol Microbiol* **32** (2): 379–391.

Ausmees, N., Jonsson, H., Hoglund, S., and Ljunggren, H., and Lindberg, M. (1999) Structural and putative regulatory genes involved in cellulose synthesis in *Rhizobium leguminosarum* bv. trifolii. *Microbiology* **145**: 1253–1262.

Blackhart, B.D., and Zusman, D. (1985) The frizzy genes of *Myxococcus xanthus* control directional movement of gliding motility. *Proc Natl Acad Sci USA* **82**: 8767–8770.

Bonner, J.T. (1982) Evolutionary strategies and developmental constraints in the cellular slime molds. *Am Nat* **119**: 530–552.

Dworkin, M. (1996) Recent advances in the social and developmental biology of the Myxobacteria. *Microbiol Rev* **60**: 70–102.

Ellehauge, E., Norregaard-Madsen, M., and Sogaard-Andersen, L. (1998) The FruA signal transduction protein provides a checkpoint for the temporal coordination of intercellular signals in *M. xanthus* development. *Mol Microbiol* **30**: 807–813.

Foster-Hartnett, D.F., and Kranz, R.G. (1994) The *Rhodobacter capsulatus glnB* gene is regulated by NtrC at tandem *rpoN*-independent promoters. *J Bacteriol* **176**: 5171–5176.

Foster-Hartnett, D., Cullen, P., Monika, E., and Kranz, R. (1994) A new type of NtrC transcriptional activator. *J Bacteriol* **176**: 6175–6187.

Gorski, L., Gronewold, T., and Kaiser, D. (2000) A sigma-54 activator protein necessary for spore differentiation within the fruiting body of *Myxococcus xanthus*. *J Bacteriol* **182**: 2438–2444.

Hagen, D.C., Bretscher, A.P., and Kaiser, D. (1978) Synergism between morphogenetic mutants of *Myxococcus xanthus*. *Dev Biol* **64**: 284–296.

Harris, B.Z., Kaiser, D., and Singer, M. (1998) The guanosine nucleotide (p)ppGpp initiates development and A-factor production in *Myxococcus xanthus*. *Genes Dev* **12**: 1022–1035.

Jelsbak, L., and Søgaard-Andersen, L. (1999) The cell-surface associated C-signal induces behavioral changes in individual *M. xanthus* cells during fruiting body morphogenesis. *Proc Nat Acad Sci USA* **96**: 5031–5036.

Jelsbak, L., and Søgaard-Andersen, L. (2000) Pattern formation: fruiting body morphogenesis in *Myxococcus xanthus*. *Curr Opin Microbiol* **3**: 637–642.

Julien, B., Kaiser, A.D., and Garza, A. (2000) Spatial control of cell differentiation in *Myxococcus xanthus*. *Proc Nat Acad Sci USA* **97**: 9098–9103.

Kaiser, D. (1979) Social gliding is correlated with the presence of pili in *Myxococcus xanthus*. *Proc Natl Acad Sci USA* **76**: 5952–5956.

Kaiser, D. (1999) Cell fate and organogenesis in bacteria. *Trends Genet* **15**: 273–277.

Kaiser, D., and Kroos, L. (1993) Intercellular signaling. In *Myxobacteria II.* Dworkin, M., and Kaiser, D. (eds). Washington, DC: American Society for Microbiology Press, pp. 257–283.

Kim, S.K., and Kaiser, D. (1990a) C-factor: a cell-cell signalling protein required for fruiting body morphogenesis of *M. xanthus*. *Cell* **61**: 19–26.

Kim, S.K., and Kaiser, D. (1990b) Cell alignment required in differentiation of *Myxococcus xanthus*. *Science* **249**: 926–928.

Kim, S.K., and Kaiser, D. (1990c) Purification and properties of *Myxococcus xanthus* C-factor, an intercellular signaling protein. *Proc Natl Acad Sci USA* **87**: 3635–3639.

Kim, S.K., and Kaiser, D. (1991) C-factor has distinct aggregation and sporulation thresholds during *Myxococcus* development. *J Bacteriol* **173**: 1722–1728.

Kingsley, D.M., Bland, A.E., Grubber, J.M., Marker, P.C., Russell, L.B., Copeland, N.G., and Jenkins, N.A. (1992) The mouse short ear skeletal morphogenesis locus is associated with defects in a bone morphogenetic member of the TGF-β superfamily. *Cell* **71**: 399–410.

Kroos, L., and Kaiser, D. (1987) Expression of many developmentally regulated genes in *Myxococcus* depends on a sequence of cell interactions. *Genes Dev* **1**: 840–854.

Kroos, L., Kuspa, A., and Kaiser, D. (1986) A global analysis of developmentally regulated genes in *Myxococcus xanthus*. *Dev Biol* **117**: 252–266.

Kruse, T., Lobendanz, S., Berthelesen, N.M.S., and

Søgaard-Andersen, L. (2001) C-signal: a cell surface-associated morphogen that induces and coordinates multicellular fruiting body morphogenesis and sporulation in *M. xanthus*. *Mol Microbiol* **39**: 1–14.

Kuhlwein, H., and Reichenbach, H. (1968) Swarming and morphogenesis in *Myxobacteria*. *Inst Wiss Film*, Film C893/1965. Gottingen, Germany.

Lee, B.-U., Lee, K., Mendez, J., and Shimkets, L.J. (1995) A tactile sensory system of *Myxococcus xanthus* involves an extracellular NAD(P)$^+$-containing protein. *Genes Dev* **9**: 2964–2973.

Li, S., Lee, B.U., and Shimkets, L. (1992) *csgA* expression entrains *Myxococcus xanthus* development. *Genes Dev* **6**: 401–410.

Licking, E., Gorski, L., and Kaiser, D. (2000) A common step for changing the cell shape in fruiting body and starvation-independent sporulation of *Myxococcus xanthus*. *J Bacteriol* **182**: 3553–3558.

O'Connor, K.A., and Zusman, D.R. (1989) Patterns of cellular interactions during fruiting-body formation in *Myxococcus xanthus*. *J Bacteriol* **171**: 6013–6024.

O'Connor, K.A., and Zusman, D.R. (1991) Development in *Myxococcus xanthus* involves differentiation into two cell types, peripheral rods and spores. *J Bacteriol* **173**: 3318–3333.

Ogawa, M., Fujitani, S., Mao, X., Inouye, S., and Komano, T. (1996) FruA, a putative transcription factor essential for the development of *Myxococcus xanthus*. *Mol Microbiol* **22**: 757–767.

Sager, B., and Kaiser, D. (1993) Two cell-density domains within the *Myxococcus xanthus* fruiting body. *Proc Nat Acad Sci USA* **90**: 3690–3694.

Sager, B., and Kaiser, D. (1994) Intercellular C-signaling and the traveling waves of *Myxococcus*. *Genes Dev* **8**: 2793–2804.

Sambrook, J., Fritsch, E.F., and Maniatis, T. (1989) *Molecular Cloning: A Laboratory Manual*, 2nd edn. Cold Spring Harbor, NY: Cold Spring Harbor Laboratory Press.

Shimkets, L., and Kaiser, D. (1982) Induction of coordinated movement of *Myxococcus xanthus* cells. *J Bacteriol* **152**: 451–461.

Shimkets, L.J., and Rafiee, H. (1990) CsgA, an extracellular protein essential for *Myxococcus xanthus* development. *J Bacteriol* **172**: 5299–5306.

Shimkets, L.J., Gill, R.E., and Kaiser, D. (1983) Developmental cell interactions in *Myxococcus xanthus* and the spoC locus. *Proc Natl Acad Sci USA* **80**: 1406–1410.

Søgaard-Andersen, L., and Kaiser, D. (1996) C-factor, a cell-surface-associated intercellular signaling protein, stimulates the cytoplasmic Frz signal transduction system in *Myxococcus xanthus*. *Proc Nat Acad Sci USA* **93**: 2675–2679.

Søgaard-Andersen, L., Slack, F., Kimsey, H., and Kaiser, D. (1996) Intercellular C-signaling in *Myxococcus xanthus* involves a branched signal transduction pathway. *Genes Dev* **10**: 740–754.

Sommer, J.M., and Newton, A. (1989) Turning off flagellum rotation requires the pleiotropic gene *pleD: pleA*, *pleC*, *and pleD* define two morphogenic pathways in *Caulobacter crescentus*. *J Bacteriol* **171**: 392–401.

Spratt, B.G., Hedge, P.J., teHessen, S., Edelman, A., and Broome-Smith, J.K. (1986) Kanamycin-resistant vectors that are analogues of plasmids pUC8, pUC9, pEMBL8, and pEMBL9. *Gene* **41**: 337–342.

Stock, A.M., Koshland, D.E., and Stock, J.B. (1985) Homologies between the *Salmonella typhimurium* CheY protein and proteins involved in the regulation of chemotaxis, membrane protein synthesis and sporulation. *Proc Nat Acad Sci USA* **82**: 7989–7993.

Wedel, A., Weiss, D.S., Popham, D., Droge, P., and Kustu, S. (1990) A bacterial enhancer functions to tether a transcriptional activator near a promoter. *Science* **248** (4954): 486–490.

White, D. (1993) Myxospore and fruiting body morphogenesis. In *Myxobacteria II*. Dworkin, M., and Kaiser, D. (eds). Washington, DC: American Society for Microbiology Press, pp. 307–332.

Wu, S.S., and Kaiser, D. (1997) Regulation of expression of the pilA gene in *Myxococcus xanthus*. *J Bacteriol* **179**: 7748–7758.